Sensors & Transducers, Vol. 169, Issue 4, April 2014, pp. 33-41

Sensors & Transducers

© 2014 by IFSA Publishing, S. L.
http://www.sensorsportal.com

Polarization Calculation and Underwater Target Detection Inspired by Biological Visual Imaging

[1] Jie Shen, [1, *] Huibin Wang, [1] Zhe Chen, [2] Yi Wei, [1] Yurong Wu
[1] College of Computer and Information Engineering, Hohai University, Nanjing, 210098, China,
[2] Institute of Communication Engineering, PLA University of Science and Technology, Nanjing, 210007, China
[*] E-mail: hbwang@hhu.edu.cn

Received: 22 January 2014 /Accepted: 7 March 2014 /Published: 30 April 2014

Abstract: In challenging underwater environments, the polarization parameter maps calculated by the Stokes model are characterized by the high noise and error, harassing the underwater target detection tasks. In order to solve this problem, this paper proposes a novel bionic polarization calculation and underwater target detection method by modeling the visual system of mantis shrimps. This system includes many operators including a polarization-opposition calculation, a factor optimization and a visual neural network model. A calibration learning method is proposed to search the optimal value of the factors in the linear subtraction model. Finally, a six-channel visual neural network model is proposed to detect the underwater targets. Experimental results proved that the maps produced by the polarization-opposition parameter is more accurate and have lower noise than that produced by the Stokes parameter, achieving better performance in underwater target detection tasks.
Copyright © 2014 IFSA Publishing, S. L.

Keywords: Polarization image, Target detection, Mantis shrimp vision, Polarization-opposition parameter, Polarization calculation.

1. Introduction

Underwater target detection is the key in underwater target identification, tracking and inspection system [1, 2]. In contrast to the ground-based images, underwater images are suffered from the attenuation and scattering by the water medium [3]. Hence, the underwater images are characterized by the low-contrast, low-SNR and high color distortion. Strategies of applying or transplanting the normal image processing method on the underwater images are unreasonable. By contrast, the based underwater polarization imaging technology not only has the ability to generate high-quality images with high-contrast, but also gives us more information about the surface of the objects [4-8]. This information is significant to the target detection for increasing the correctness and efficiency [9].

The Stokes vector which is proposed by the G. G. Stokes takes four parameters, as I, Q, U and V, to model the polarization feature. These four parameters are the time-average moderation on the light intensity and can be directly or indirectly given by the imaging-metrics [10, 11]. However, since the nature of the wavelength-selective transmittance, the non-homogeneous transmittance or the incorrect operation of the polarizer, the error of measurement all would cause the error in Stokes parameter calculation and produce the noise in the result.

Moreover, although the polarization imaging technology in the underwater environments has the ability to reduce the background noise, the light reflected by objects at the same time is filtered. This nature hazes the underwater polarization images, making the underwater target detection extraction and recognition difficult. In order to enhance the polarization maps, many methods such as the multi-angle measuring, image filtering or image fusing are proposed [12, 13]. According to the multi-angle measurement technology, N polarization maps are collected in the 360°. N/2 sets of the Stokes parameters are calculated and averaged to produce a consequent Stokes parameter map. However, this technology can merely reduce the error causing by rolling the polarizer but can not reduce the noise of the polarization maps. Image filtering is to smooth the polarization image by removing the noise. However, this method would distort the edge or the detail information in the maps. Image fusion is to operate multi-level wavelet decomposition on the polarization image, the coefficient of each level is given and fusion. Finally the polarization parameters are calculated by the reconstruction of the fused coefficients. For this method, the discipline of the coefficient fusion is the key, which is complicated with high time cost. To solve the problems above, this paper is proposed with the topic that how to efficient extract the polarization information for enhancing the performance of the underwater target detection.

In the underwater world, many animals have strong ability to sense and use the polarization information for adapting to the low-intensity and high scattering effect in the optical environments [14]. This biological visual mechanism provides us a valuable sample. Inspirited by this mechanism, a novel polarization calculation and modeling method is proposed for the task of underwater target detection. Experimental results given by the proposed method demonstrated the increased correctness of the target detection and the enhanced contrast between the target and the background.

2. Polarization-opposition Perception

2.1. The Compound Eye of Mantis Shrimps

Mantis shrimps possess typical apposition compound eyes which have more types of photoreceptor types than any other animal. The compound eyes are consisted of ommatidia with eight photoreceptors [15, 16]. The compound eye can be sub-divided into three morphologically discrete regions, a mid-band with six rows and dorsal and ventral hemispheres (Fig. 1). The eye has a 12-channel color vision, a 2-channel circular polarization vision, and a multi-channel linear polarization vision.

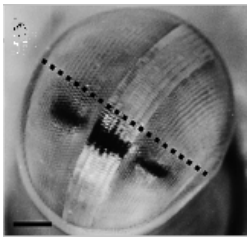

Fig. 1. The eye of mantis shrimp.

2.2. Polarization-opposition Mechanism

Each ommatidium in the compound eyes of mantis shrimp is composed of eight photoreceptor cells, labeled by R1, R2, …, R8. Because of electrophysiological experiment, the R1-R7 cells are subdivided into two groups (Group I and Group II) in the hemispheres and rows 5 and 6. Group I cells, labeled R1, R4 and R5, have orthogonal e-vector with Group II cells, labeled R2, R3, R6 and R7 [17]. Photoreceptors of the two groups are sensitive to linear polarized light. The same point in space is examined by an ommatidium in the ventral hemisphere, with e-vector vertical and horizontal, and an ommatidium in the dorsal hemisphere with e-vector at +45° and -45° [15].

The intensity information of polarization light with various polarization angels is inputted into the visual system and a pair of the input of the orthogonal polarization forms an antagonist. The output is generated by the opposition calculation in an antagonistic pair, which in this paper is call of the polarization sensitivity. From the mechanism shown in Fig. 2 the output of the system is comprised of a polarization sensitivity with four various polarization angles as 0°, 45°, -45° and 90°. For simplification, the four parameters are generally called as opponent polarization parameters [18].

The mechanism above is call of the polarization-opposition mechanism, which can not only enhance the response to the polarization, increasing the polarization sensitivity of the compound eye, but also reduce the influence of the optical noise on the polarization information.

3. Polarization-opposition Model

The polarization-opposition perception of the mantis shrimps is based on the difference of the polarization intensity in the orthometric e vector. There are four antagonistic pairs in the visual system of mantis shrimps, the E vector are respectively assigned with four angles as 0°~90°, 90°~0°, 45°~-45° and -45°~45°. One output of the antagonistic pairs would inhibit the output from another channel. Hence an opposition mechanism is formed and call of the polarization-opposition perception mechanism in this paper. This system can be described as Fig. 2.

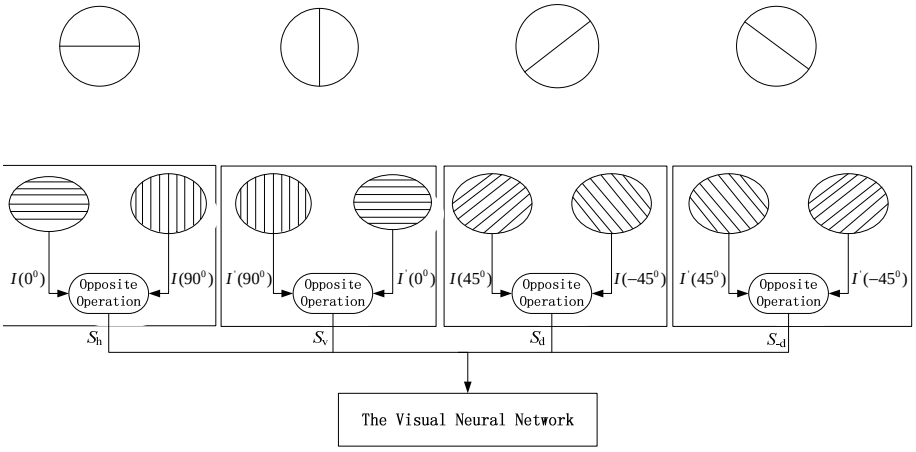

Fig. 2. The polarization-opposition model.

An opponent perception model in this paper is established by imitating the opponent perception mechanism of the mantis shrimps as shown in Fig. 3. This linear model is formed by a typical subtraction function. The input is a pair of antagonistic polarization parameters and the output is the difference of this pair of the polarization signal. Moreover, there are two factors for controlling the moderation of the antagonistic signal. The model is formulated as:

$$S_{\theta_1-\theta_2} = k_{\theta_1} * I(\theta_1) - k_{\theta_2} * I(\theta_2) \quad (1)$$

where $I(\theta_1)$ and $I(\theta_2)$ are the intensity of the polarization light with the E vector at the angle of θ_1 and θ_2, respectively and θ_1, θ_2 must meet the condition $\theta_1 + \theta_2 = 90^0$ to ensures the antagonistic relation. k_{θ_1} $\left(k_{\theta_1} \geq 1\right)$ and k_{θ_2} $\left(0 < k_{\theta_2} \leq 1\right)$ are the weighting factors for controlling the moderation on every signal and simulating the different sensitivity in different polarization angles. The moderation factor has strong influence on the output and determinates the quality of the polarization-opponent maps. However, since the lack of the relative biological study a certain value is not given in this chapter but will be discussed in the experiments.

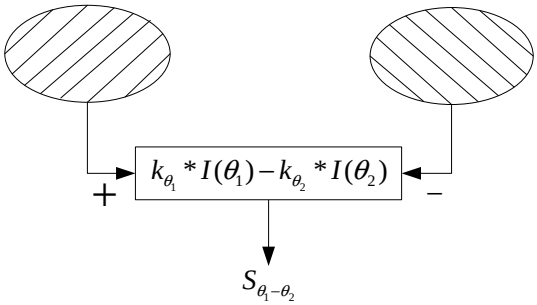

Fig. 3. The mathematic model of opponent perception.

4. Underwater Target Detection

To efficiently detect the underwater targets, we firstly imitate the polarization-opposition mechanism of the mantis shrimps to calculate the polarization-opposition maps, polarization-pattern maps and the light intensity maps. Then the machine learning method is introduced to optimize the moderation factors in the model. At last various maps are inputted into the neural network to detect the underwater targets. The framework of the proposed underwater target detection method is shown in Fig. 4.

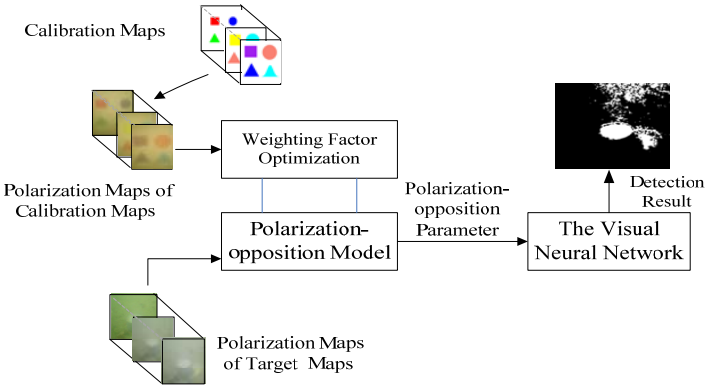

Fig. 4. The framework of the underwater target detection.

4.1. Opponent Model Based Polarization Parameter Calculation

1) Polarization-opposition parameter.

The inputs of polarization-opposition model are the intensity of the polarization, labeled as $I(0^0)$, $I(90^0)$; $I^{'}(0^0)$, $I^{'}(90^0)$; $I(45^0)$, $I(-45^0)$ and $I^{'}(45^0)$, $I^{'}(-45^0)$. According to the equation 1 the output signal can be described as:

$$S_h = k_1 * I(0^0) - k_2 * I(90^0) \tag{2}$$

$$\begin{aligned} S_v &= k_3 * I^{'}(90^0) - k_4 * I^{'}(0^0) \\ &= k_3 * I(90^0) - k_4 * I(0^0) \end{aligned} \tag{3}$$

$$S_d = k_5 * I(45^0) - k_6 * I(-45^0) \tag{4}$$

$$\begin{aligned} S_{-d} &= k_7 * I^{'}(-45^0) - k_8 * I^{'}(45^0), \\ &= k_7 * I(-45^0) - k_8 * I(45^0) \end{aligned} \tag{5}$$

where parameters S_h, S_v, S_d and S_{-d} denote the polarization-opposition parameter specialized to the polarization with the angle of 0°, 90°, 45° and -45°. k_1, k_2, …, k_8 are the moderation factors, denoting the enhancement or the inhabitation on the intensity of the polarization. In the ideal case, $I(0^0) = I^{'}(0^0)$, $I(0^0) = I^{'}(0^0)$, $I(45^0) = I^{'}(45^0)$, $I(-45^0) = I^{'}(-45^0)$.

In addition, from the function $I(0^0) + I(90^0) = I(45^0) + I(-45^0)$ the opponent-polarization sensitivity parameters at 45° and -45° can be calculated as:

$$\begin{aligned} S_d &= k_5 * I(45^0) - k_6 * I(-45^0) \\ &= k_5 * I(45^0) - k_6 * (I(0^0) + I(90^0) - I(45^0)) \\ &= (k_5 + k_6) * I(45^0) - k_6 * (I(0^0) + I(90^0)) \end{aligned} \tag{6}$$

$$\begin{aligned} S_{-d} &= k_7 * I(-45^0) - k_8 * I(45^0) \\ &= k_7 * (I(0^0) + I(90^0) - I(45^0)) - k_8 * I(45^0) \\ &= k_7 * ((I(0^0) + I(90^0)) - (k_7 + k_8) * I(45^0) \end{aligned} \tag{7}$$

Thus, the polarization-opposition parameter maps describing the target can be calculated.

2) Degree of polarization.

The partial polarized light I_o can be expressed as the summation of the natural light I_n and the plane polarized light I_p:

$$I_o = I_n + I_p \tag{8}$$

Thus, when a beam of light with the intensity I pass through an ideal polarizer and the angle between the polarizer and the optical axis is θ, the intensity of polarization light $I^{'}$ can be calculated as:

$$\begin{aligned} I^{'}(\theta) &= I_n^{'}(\theta) + I_p^{'}(\theta) = \frac{1}{2} I_n + I_p \cos^2 \theta \\ &= \frac{1}{2}(I - I_p) + I_p \cos^2 \theta = \frac{1}{2} I + \frac{1}{2} I_p \cos 2\theta \end{aligned} \tag{9}$$

The degree of polarization is the proportion of the polarization intensity to the total light intensity. Hence, the degree of polarization $DoP = \frac{I_p}{I}$, according to the equation 9 can be expressed as:

$$\begin{aligned} I^{'}(\theta) &= \frac{1}{2} I + \frac{1}{2} I * DoP \cos 2\theta \\ &= \frac{1}{2} I(1 + DoP \cos 2\theta) \end{aligned} \tag{10}$$

Given two polarization sensitivity parameters S_h and S_v, as:

$$\begin{aligned} S_h &= k_1 I(0^0) - k_2 I(90^0) \\ &= k_1 (\frac{1}{2} I(1 + DoP)) - k_2 (\frac{1}{2} I(1 - DoP)) \\ &= \frac{1}{2} I(k_1 + k_1 DoP - k_2 + k_2 DoP) \end{aligned} \tag{11}$$

$$\begin{aligned} S_v &= k_3 I(90^0) - k_4 I(0^0) \\ &= k_3 (\frac{1}{2} I(1 - DoP)) - k_4 (\frac{1}{2} I(1 + DoP)) \\ &= \frac{1}{2} I(k_3 - k_3 DoP - k_4 - k_4 DoP) \end{aligned} \tag{12}$$

The degree of polarization (DoP) can be calculated by combining the equation (11) and equation (12):

$$DoP = \frac{M(k_3 - k_4) - (k_1 - k_2)}{M(k_3 + k_4) + (k_1 + k_2)}, \tag{13}$$

where $M = \frac{S_h}{S_v}$.

3)Synthetic light intensity parameter

The synthetic light intensity can be calculated as:

$$I = I(0^0) + I(90^0) = I(45^0) + I(-45^0) = \frac{S_v + S_h}{k_1 - k_2} \tag{14}$$

4.2. Weighting Factor Optimization

As aforementioned, the value of the weighting factor has strong influence on the quality of the polarization-opposition maps. In this paper, the machine learning based methods are used for the optimization process, and the optimal solution is given by the Gaussian curve fitting.

4.2.1. Calibration Maps

36 calibration maps are designed as the training data as shown in Fig. 5. These calibration maps are varied with color (including red, orange, yellow, green, cyan, blue, purple, black) and shapes (rectangular, circular, triangular, Gaussian). The calibration maps are set underwater for polarization imaging to acquire the polarization maps with three different polarization angles.

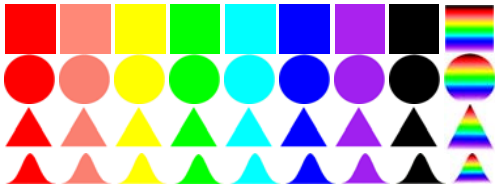

Fig. 5. The training maps.

4.2.2. Weighting Factor Optimization

Base of the Biological experiment[18], the value of the parameters k_1 is varied in the interval of [1,15], the optimal step is 0.5, while the parameter k_2 is varied in the interval of $[0.1,1]$, the step is 0.1. Based on the equation 2, the polarization sensitive maps in the horizontal orientation are calculated. Then the information entropy $E(k_1,k_2)$ for these polarization maps can be calculated as:

$$E=-\sum_{i=0}^{L-1}P(i)\log_2(P(i)), \quad (15)$$

where 0, 1, …, L-1 are the level of the gray of the polarization image. P(i) is the ratio of the pixel with the intensity of I. When the parameter of information entropy $E(k_1,k_2)$ is maximized, the image includes the most abundant scenes information, and images are of the highest quality. Hence, the maximal value of the $E(k_1,k_2)$ is in line with the optimal value of the weights k_1 and k_2, denoting as k_1^b and k_2^b, respectively. The flow chart of the optimization algorithm is shown in Fig. 6.

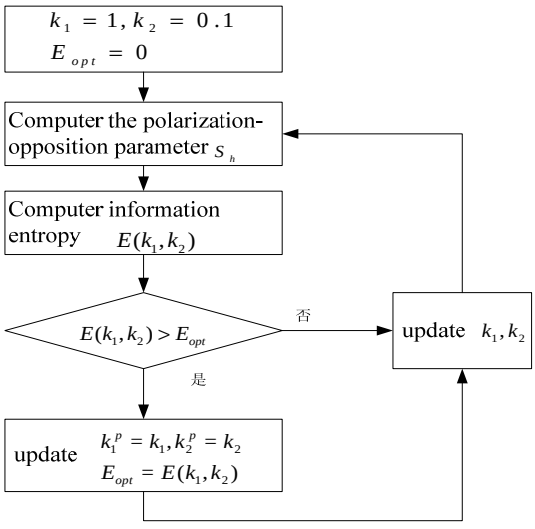

Fig. 6. The flow chart of weighting factor optimization.

4.3. Visual Neural Network

The neural network inspirited by the visual system of mantis shrimps [19] is applied for detecting the underwater target. These neuron models are jointly to form the neural network with six-channel input in this detection framework.

5. Experiment Results and Analysis

5.1. Experimental Data Collection and Optimization of the Weights

By using the polarization imaging system the training data is collected at three polarization angle on a sunny day. The visibility is less than 80 cm and the background is green. With the equation (2), (3), (6) and (7), the opponent polarization parameter maps (S_h, S_v, S_d and S_{-d}) are given in Fig. 5. Then, the degree of the polarization (DoP) and the intensity pictures (I) are calculated. By the optimization process, the optimal value of the weights is given as shown in the Table 1 and Table 2.

Table 1. The distribution interval of weighting factors k_1, k_3, k_5 and k_7.

	K_1	K_3	K_5	K_7
1~2	0	0	0	2
2~3	4	0	0	13
3~4	12	2	0	11
4~5	6	4	2	6
5~6	4	12	2	4
6~7	4	8	4	0
7~8	2	2	8	0
8~9	2	2	10	0
9~10	0	2	6	0
10~11	0	2	4	0
11~12	1	0	0	0

Table 2. The distribution interval of weighting factor k_2, k_4, k_6 and k_8.

	k_2	k_4	k_6	k_8
0.1~0.2	0	0	0	1
0.2~0.3	0	0	0	1
0.3~0.4	0	0	0	0
0.4~0.5	0	0	0	5
0.5~0.6	0	0	0	6
0.6~0.7	0	4	0	16
0.7~0.8	0	0	4	0
0.8~0.9	2	4	0	6
0.9~1.0	34	28	32	1

The histogram of each weight is fitted by the Gaussian model and the center is selected as the representation to the value of the weight as shown in Fig. 7.

From the Fig. 7, different parameters are assigned with different values. The representations of the optimal value are k_1=3.692, $k_2=0.8716$, $k_3=5.236$, $k_4=0.8667$, $k_5=7.317$, $k_6=0.9$, $k_7=2.667$ and $k_8=0.5685$.

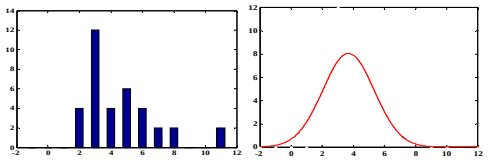

(a) k_1

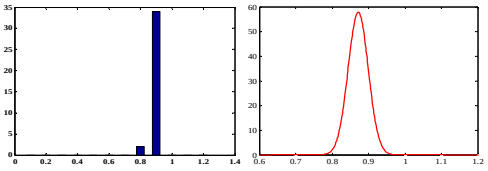

(b) k_2

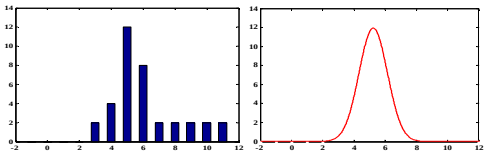

(c) k_3

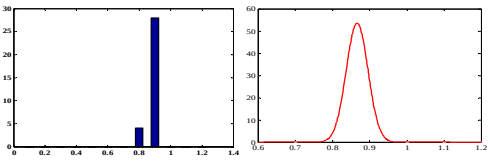

(d) k_4

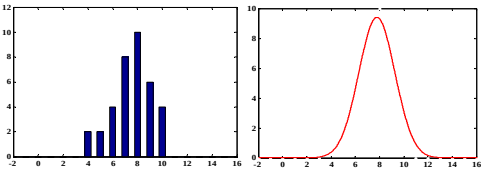

(e) k_5

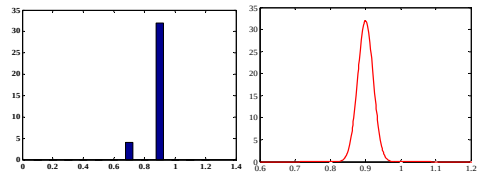

(f) k_6

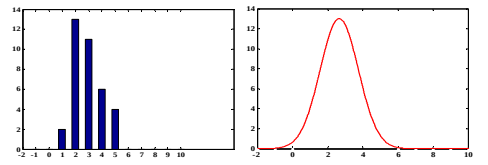

(g) k_7

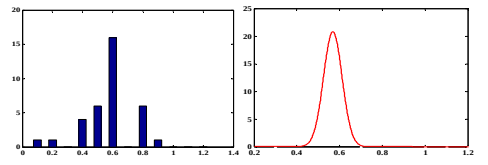

(h) k_8

Fig. 7. The histogram and Gaussian fitting of weighting factor.

5.2. Comparison of Polarization-opposition Parameters and Stokes Polarization Parameters

To evaluate the proposed the polarization-opposition parameter, the Stokes parameter is selected as the reference. The performance in characterizing the target's polarization information is estimated. A set of the underwater polarization images is acquired and used in the following experiments. In the underwater environment, three polarization images of the iron box and the coin at three different polarization angle are collected as shown in Fig. 8 (a)-(c) and Fig. 11 (a)-(c).

The maps produced by the polarization-opposition parameter, the degree of polarization and the light intensity maps are shown in Fig.8 (d) ~ Fig. 8 (i) and Fig. 11 (d) ~ Fig. 11 (i). Stokes parameters maps, the degree of polarization and the light intensity images are shown in Fig. 9 (a) ~ Fig. 9 (d) and Fig. 12 (a) ~ Fig. 12 (d). By the images enhancement method, the Stokes parameter map, the degree of polarization map and the light intensity map are shown in Fig. 10 (a) ~ Fig. 10 (d) and Fig. 10 (a) ~ Fig. 13 (d). By contrast, the parameter Sh and the parameter Sv have the equivalence performance on presenting the physical material of the targets, while the parameter Sd and the parameter S-d have the abundant information about the edge and the contour of the targets. By comparing the Fig. 9, Fig. 10, Fig. 12 and Fig. 13, the homomorphic filtering has significant performance on stretching the contrast between the target and the background. Moreover, by contrast, the maps of the polarization-opposition parameter have more information about the object and can stretch the contrast between the object and the background.

(a) $I(0^0)$ (b) $I(45^0)$ (c) $I(90^0)$

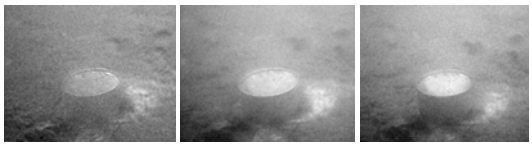

(d) S_h (e) S_v (f) S_d

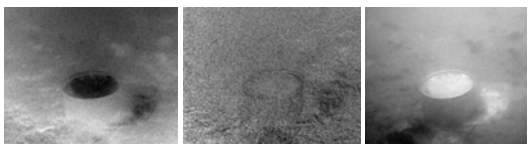

(g) S_{-d} (h) DoP (i) I

Fig. 8. The polarization, the polarization-opposition parameter, the degree of polarization and the light intensity maps of the iron box.

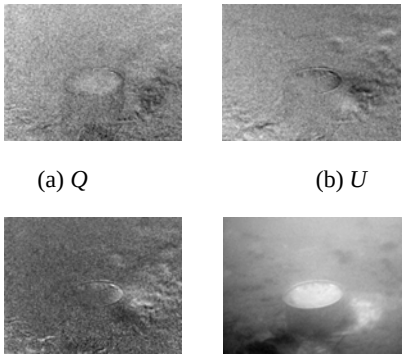

(a) *Q* (b) *U*

(c) *DoP* (d) *I*

Fig. 9. The Stokes' polarization parameter, the degree of polarization and the light intensity maps of the iron box.

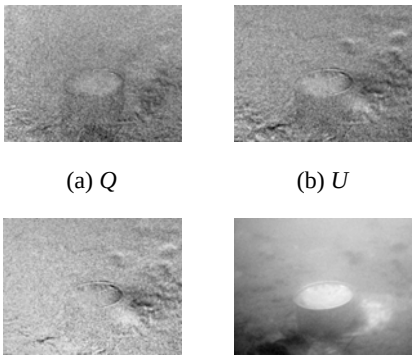

(a) *Q* (b) *U*

(c) *DoP* (d) *I*

Fig. 10. The Stokes' polarization parameter, the degree of polarization and the light intensity maps of the iron box after polarization-preprocessing.

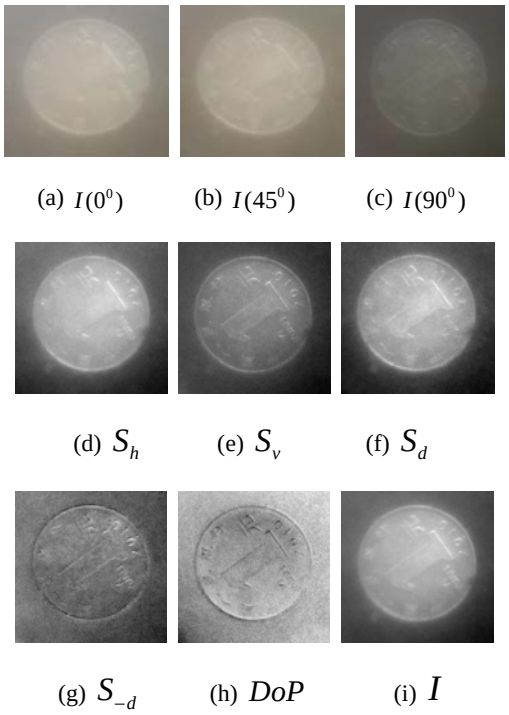

(a) $I(0^0)$ (b) $I(45^0)$ (c) $I(90^0)$

(d) S_h (e) S_v (f) S_d

(g) S_{-d} (h) DoP (i) I

Fig. 11. The polarization, the polarization-opposition parameter, the degree of polarization and the light intensity maps of the coin.

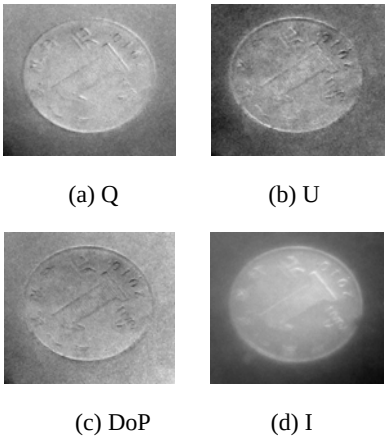

(a) Q (b) U

(c) DoP (d) I

Fig. 12. The Stokes' polarization parameter, the degree of polarization and the light Intensity maps of the coin.

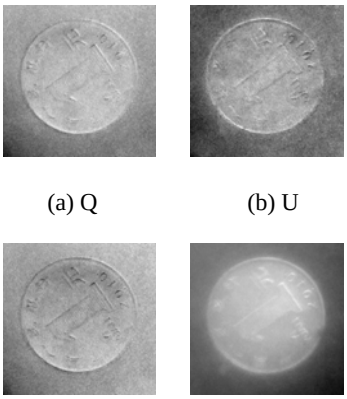

(a) Q (b) U

(c) DoP (d) I

Fig. 13. The Stokes' polarization parameter, the degree of polarization and the light intensity maps of the coin after polarization-preprocessing.

5.3. Target Detection

The target detection results are shown in Fig. 14(a), Fig. 15(a), Fig. 14(b) and Fig. 15(b) respectively.

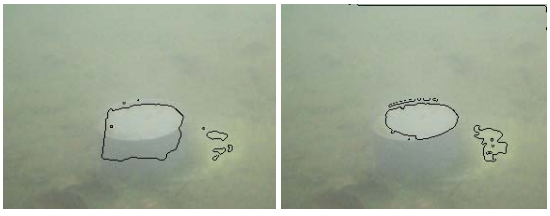

(a) Base of Polarization-opposition Parameter (b) Base of Stokes' Polarization Parameter

Fig. 14. The result of target detection in depth 50 cm.

The evaluation is operated by the following standard:

$$C_{good} = \frac{\Omega_{in} \bigcap \Omega_o}{\Omega_o} \quad (16)$$

$$C_{false} = \frac{\Omega_{in} \bigcap \Omega_b}{\Omega_b}, \quad (17)$$

where Ω_{in} is the internal region of the extracted area, Ω_o is the region of the object to be detected, and Ω_b is the background region. C_{good} is the ratio of the correct extraction in the true object region, while C_{false} is the ratio of the false extraction in the background region. Obviously, the larger the value of C_{good} is and the smaller the value of C_{false} is, the more robust algorithm we gain.

From the Table 3 in the swallow water, the target can be extracted by the polarization image, while in the deeper water since the water medium seriously decrease the quality of the polarization maps the contrast between the target and the background is decreased, decreasing the correctness of the target detection. However, in this case, the polarization-opposition maps with lower noise have the ability to enhance the result of the underwater object detection.

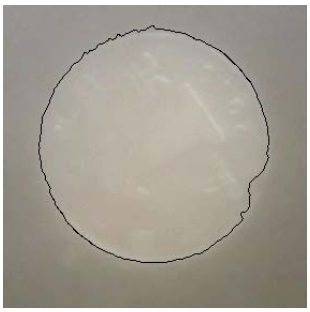

(a) Base of Polarization-opposition Parameter

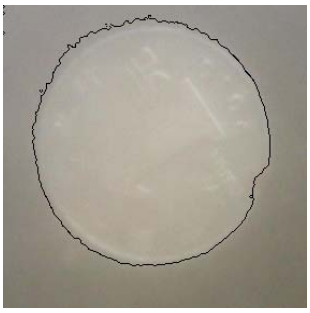

(b) Base of Stokes' Polarization Parameter

Fig. 15. The result of target detection in depth 20 cm.

Table 3. The quantitative evaluation of target detection in underwater.

	C_{good}	C_{false}
Fig. 14(a)	87.93 %	0.64 %
Fig. 14(b)	44.52 %	1.04 %
Fig. 15(a)	94.73 %	0.86 %
Fig. 15(b)	93.29 %	1.75 %

6. Conclusion

By imitating the polarization vision of mantis shrimp this paper proposed a novel polarization parameter to describe the target polarization information. By this parameter, better performance of target detection is achieved in contrast to the Stokes parameters. By combining the optics theory, biological researches and the machine learning method, a linear weighting subtraction model is proposed to imitate the polarization vision of mantis shrimps. However, due to the limitation of the biological study, the weights can only be obtained by machine learning method which is likely to be affected by the quality of water, depth of imaging, distance of imaging and weather, etc. In practice, the underwater optical environment is complicated and variable. Therefore, in the further work, we should not only specialize to any single underwater environment, but also establish the dynamic relation for various underwater optical environments, which can increase the generalization of the proposed algorithm.

References

[1]. L. F. Gian, Visual inspection of sea bottom structures by an autonomous underwater vehicle, *IEEE Transactions on Systems, Man and Cybernetics, Part B*, Vol. 31, Issue 5, 2001, pp. 691-705.

[2]. Q. Wang, X. W. Wang, X. Pan, Adaptive sonar beamformer based on inverse QR decomposition and recursive least squares filter for underwater target detection, *International Journal of Remote Sensing*, Vol. 33, Issue 13, 2012, pp. 3987-3998.

[3]. T. Treibitz, Y. Y. Schechner, Active polarization descattering, *IEEE Transactions on Pattern Analysis and Machine Intelligence*, Vol. 31, Issue 3, 2009, pp. 385-399.

[4]. R. Shirvany, M. Chabert, J. Y. Tourneret, Estimation of the degree of polarization for hybrid/compact and linear Dual-Pol SAR intensity images: principles and applications, *IEEE Transactions on Geoscience and Remote Sensing*, Vol. 51, Issue 1, 2013, pp. 539-551.

[5]. L. B. Wolff, Polarization-based material classification from specular reflection, *IEEE Transactions on Pattern Analysis and Machine Intelligence*, Vol. 12, Issue 1, 1990, pp. 1059-1071.

[6]. L. B. Wolff, Surface orientation from polarization images, in *Proceeding of the Optics, Illumination and Image Sensing for Machine Vision II*, Vol. 850, 1987, pp. 110-121.

[7]. L. B. Wolff, Polarization vision: a new sensory approach to image understanding, *Image and Vision Computing*, Vol. 15, Issue 2, 1997, pp. 81-93.

[8]. H. Chen, L. B. Wolff, Polarization phase-based method for material classification and object recognition in computer vision, in *Proceeding of the IEEE Computer Society Conference on Computer Vision and Pattern Recognition (CVPR'96)*, San Francisco, USA, 18-20 June, 1996, pp. 128-135.

[9]. J. V. Spiegel, N. Engheta, X. T. Wu, Polarization image sensors: learning from biology to make the invisible visible, in *Proceedings of the IEEE*

International Conference on Electron Devices and Solid State Circuit (EDSSC), Bangkok Thailand, 3-5 December, 2012, pp. 1-3.
[10]. Y. B. Liao, Polarization optics, *Science Press*, 2013.
[11]. Y. Q. Zhao, Imaging spectropolarimetric remote sensing and application, Xiong Si-Hua, *National Defence Industry Press*, 2011.
[12]. Y. Q. Zhao, Q. Pan, Y. C. Chen, Clutter reduction based on polarization imaging technology and image fusion theory, *Chinese Journal of Electronics*, Vol. 33, Issue 3, 2005, pp. 433-435.
[13]. Y. Q. Zhao, Q. Pan, H. C. Zhang, New polarization imaging method based on spatially adaptive wavelet image fusion, *Optical Engineering*, Vol. 45, Issue 12, 2006, Article Number: 123202.
[14]. T. W. Cronin, N. Shashar, R. L. Caldwell, Polarization vision and its role in biological signaling, *Integrative Comparative Biology*, Vol. 43, Issue 4, 2003, pp. 549-558.
[15]. N. J. Marshall, T. W. Cronin, S. Kleinlogel, Stomatopod eye structure and function: A review, *Arthropod Structure & Development*, Vol. 36, 2007, pp. 420-448.
[16]. T. H. Chiou, S. Kleinlogel, T. W. Cronin, Circular polarization vision in a stomatopod crustacean, *Current Biology*, Vol. 18, Issue 6, 2008, pp. 429-434.
[17]. S. Kleinlogel, N. J. Marshall, Electrophysiological evidence for linear polarization sensitivity in the compound eye of the stomatopod crustacean Gonodactylus chiragra, *Journal of Experiment Biology*, Vol. 209, Issue 21, 2006, pp. 4262-4272.
[18]. Samuel D. Ramsden, Leslie Anderson, Martina Mussi, Maarten Kamermans, and Craig W. Hawryshyn, Retinal processing and opponent mechanisms mediating ultraviolet polarization sensitivity in rainbow trout, *Journal of Experimental Biology*, Vol. 211, Issue 9, 2008, pp. 1376-1385.
[19]. H. B. Wang, Y. R. Wu, J. Shen, Z. Chen, Research on underwater polarization image segmentation inspired by biological optic nerve, in *Proceedings of the 2nd International Conference on Computer Science and Electronics Engineering*, Hangzhou, China, 25-26 May 2013, pp. 2178-2184.

2014 Copyright ©, International Frequency Sensor Association (IFSA) Publishing, S. L. All rights reserved. (http://www.sensorsportal.com)

International Frequency Sensor Association (IFSA) Publishing

Digital Sensors and Sensor Systems: Practical Design

Sergey Y. Yurish

The goal of this book is to help the practicians achieve the best metrological and technical performances of digital sensors and sensor systems at low cost, and significantly to reduce time-to-market. It should be also useful for students, lectures and professors to provide a solid background of the novel concepts and design approach.

Book features include:

- Each of chapter can be used independently and contains its own detailed list of references
- Easy-to-repeat experiments
- Practical orientation
- Dozens examples of various complete sensors and sensor systems for physical and chemical, electrical and non-electrical values
- Detailed description of technology driven and coming alternative to the ADC a frequency (time)-to-digital conversion

Formats: printable pdf (Acrobat) and print (hardcover), 419 pages

ISBN: 978-84-616-0652-8,
e-ISBN: 978-84-615-6957-1

Digital Sensors and Sensor Systems: Practical Design will greatly benefit undergraduate and at PhD students, engineers, scientists and researchers in both industry and academia. It is especially suited as a reference guide for practicians, working for Original Equipment Manufacturers (OEM) electronics market (electronics/hardware), sensor industry, and using commercial-off-the-shelf components

http://sensorsportal.com/HTML/BOOKSTORE/Digital_Sensors.htm